What determines the number and the timing of pulses in afternoon precipitation in the Green Ocean Amazon (GoAmazon) observations?

Yang Tian[1,2*], Yunyan Zhang[1], and Stephen A. Klein[1]

[1] Lawrence Livermore National Laboratory, Livermore, California, USA

[2] National Center for Atmospheric Research, Boulder, Colorado, USA

[*]Corresponding author: Yang Tian (yangtianharvard@gmail.com)

Key Points:

- Double pulses of afternoon precipitation are observed over the Amazon rainforest and associated with locally generated deep convective systems
- On the days with double pulses, the early-morning free troposphere is drier than that on days with a single pulse, which retards the development of convection and rain intensity
- The second precipitation pulse is connected to the first primarily through the natural selection of favorable convective clusters and the interaction between clusters

This article has been accepted for publication and undergone full peer review but has not been through the copyediting, typesetting, pagination and proofreading process, which may lead to differences between this version and the Version of Record. Please cite this article as doi: 10.1029/2021GL096075.

Abstract

Using GoAmazon observations over the central Amazon, we investigate double-pulse events of afternoon precipitation for the first time. Relative humidity is the dominant factor in determining the onset timing and the number of pulses of precipitation. A moister free troposphere on single-pulse days features heavy precipitation in the early afternoon, which stabilizes the atmosphere and prohibits further convection. On early-onset double-pulse days, weaker precipitation from shallower convection in the first pulse leads to less consumption of atmospheric instability, making the environment favorable for a second pulse of stronger precipitation. A cluster tracking algorithm using the scanning radar reflectivity is developed to examine the relationship between precipitation pulses. Through explicitly tracking convective clusters that exist from the first to the second pulse, convective aggregation plays a more dominant role to the survival of clusters with larger final size, and on average around 20% of cluster survivals are due to natural growth.

Plain Language Summary

We use observations to investigate the factors that control the timing and the number of pulses in precipitation over the central Amazon. We develop a cluster tracking algorithm to understand the mechanism of the relationship between different pulses. Free troposphere relative humidity is important in determining both precipitation onset timing and the number of pulses of precipitation. Natural selection of more favorable convective clusters and the interactions among convective clusters contribute to a second precipitation pulse.

1 Introduction

Moist convection plays an important role in the global climate system by vertically redistributing heat, moisture, momentum, and chemical species. Diurnal cycle, as one of the dominant and fastest modes of tropical variability (Sato et al. 2009), is closely tied to the global energy budget and water cycle. Despite recent progress in representations of moist convection in general circulation models (GCMs), the diurnal cycle of convection over land remains a challenge that precipitation peaks tend to occur almost in phase with surface fluxes, usually a few hours earlier compared to observations (Yang and Slingo 2001; Betts and Jakob 2002; Dai and Trenberth et al. 2004; Schlemmer et al. 2011; Yin and Porporato 2017; Christopoulos and Schneider 2021; Collier and Bowman 2004; Rosa and Collins 2013; Flato et al. 2014; Covey et al. 2016). Convection parameterization is revealed as the main source of biases in precipitation (Betts and Jakob 2002; Bechtold et al. 2004; Guichard et al. 2004; Lee et al. 2008; Pearson et al. 2014; Xie et al. 2019). Convection-permitting models improve the simulation of convection, but deficiencies still exist when compared to radar observations (Prein et al. 2015; Clark et al. 2016). Several factors come into play to determine the diurnal timing of convection over land in addition to the local driving mechanism of surface fluxes and early morning environmental conditions (e.g. atmospheric moisture, Zhuang et al. 2017). One important yet largely neglected factor in parameterizations is the interaction among the evolving convective clusters (e.g., cold pools, gravity waves, convective aggregation), on which observational studies are lacking to support theoretical development (Muller and Bony 2015; Holloway et al. 2017).

Using observations from the US Department of Energy (DOE) Atmospheric Radiation Measurement (ARM) Green Ocean Amazon (GoAmazon) field campaign, Tian et al. (2021) identified deep convective days dominated by surface-forced locally generated systems and found that the composite daytime domain mean precipitation often exhibits double pulses in the afternoon (see Figure

3c in Tian et al. 2021). Such double-pulse phenomenon is more complicated than previously observed ones at the mid-latitude land (e.g., Zhang and Klein, 2010) and can be the effect of several possibilities, e.g., composites of days with a single pulse of different timings such as one in the early afternoon and the other in the late afternoon, or composites of days with two or more consecutive precipitation pulses in the afternoon. To our best knowledge, no previous studies have examined double precipitation pulsed events in GoAmazon observations.

In this study, we aim to understand the factors determining the diurnal timing of precipitation pulses, the underlying mechanisms leading to single or double pulses, and the relationship between the consecutive pulses. On one hand, we hope that the results of this study can be used to validate the fidelity of models in representing diurnal cycle; on the other hand, this study may inform the design of a more reliable convective scheme. For example, this double-pulse phenomenon may be related to the evolution of convective clusters and their interactions, such as convective aggregation, which will be elaborated from observations in the following.

2 Data and Methods

In this study, we focus on the daytime (0800-1800 Local Standard Time (LST)) locally generated deep convective activities using ARM data during the GoAmazon field campaign (Jan. 2014 - Dec. 2015). The analysis domain is a circle with a 75-km radius centered at T3 site. All the data are publicly available at https://www.arm.gov/research/campaigns/amf2014goamazon.

2.1 ARM Observations

Vertical profiles of cloud fraction are from the merged Radar Wind Profiler (RWP) and W-band Cloud Radar (WACR) Active Remote Sensing of Cloud (ARSCL) cloud mask data product (Giangrande et al., 2016) collected at the T3 site. Precipitation is retrieved from the reflectivity of the ground-based

Sistema de Proteção da Amazônia (SIPAM) S-band scanning radar located at Manaus (Schumacher and Funk 2018). We use the 12-min gridded data with a horizontal resolution of 1.8 km and a vertical resolution of 500 meters. The reflectivity data are also used to characterize convective clusters, e.g., cluster area and echo top height. In the following, rain rate usually refers to the average precipitation within the analysis domain.

Vertical profiles of temperature and relative humidity are taken from balloon radiosondes. Convective Available Potential Energy (CAPE) and Convective Inhibition (CIN) are computed using sounding data assuming reversible adiabatic ascent of the boundary layer air parcels with the largest θ_e in the lowest 500 m (Stull 2017). Surface sensible and latent heat fluxes are from the hourly averaged Quality Controlled Eddy Correlation (QCECOR) Flux Measurement. Planetary Boundary Layer (PBL) heights are defined as the daytime convective mixed-layer top using the doppler-lidar measured 10-min vertical velocity variances with a threshold value of 0.06 m^2s^{-2} (Tian et al. 2021).

2.2 Classification of local deep convection days based on precipitation pulses

We use the convective classification algorithm of Tian et al. (2021), by which 126 locally generated deep convection days are selected primarily based upon the occurrence of daytime maximum cloud/echo top heights exceeding 7 km. Here the locally generated deep system refers to the daytime surface-forced local convection originated in the analysis domain without the influence from large-scale forcing (e.g. MCSs). To investigate the underlying mechanisms controlling the pulses of precipitation, we stratify days by the timing of precipitation onset as well as the number of pulses of precipitation. We first divide these days into two broad categories: days with the first precipitation pulse before and after 1400 LST based on Figure 3c in Tian et al. (2021), which we call “early” and “late” onset days respectively. Within each of these two categories, days with a single precipitation pulse are further

distinguished from those with multiple pulses (usually two), which we call "single" and "double" pulse days. From the 12-minute time-series of rain rates, we define a pulse as occurring when the local maximum exceeds 0.15 mm/hr and is at least 0.05 mm/hr larger than the 12-minute precipitation immediately before and after. We further require that every pulse is separated from another pulse by at least two timesteps (36 minutes) to ignore small oscillations. Thus, there are four categories: 21 early-onset single-pulse (early single) days, 35 early-onset double-pulse (early double) days, 32 late-onset single-pulse (late single) days, and 14 late-onset double-pulse (late double) days. These days in total consist of 81% of all the locally generated deep convection days defined in Tian et al. (2021), thus are considered representative of a majority of locally generated deep convection days. Figure 1 shows the diurnal cycle of the vertical profile of cloud fraction and the rain rate averaged over all the days in each of the four categories. On days with early precipitation onset, the maximum rain rate occurs around 1330 LST on the early single days (Fig. 1a) with a value larger than those of the first (1300 LST) and the second pulses (1530 LST) on the early double days (Fig. 1b). On days with late precipitation onset, the maximum rain rate occurs about 1600 LST on late single days with a value comparable to that of the first pulse (1500 LST) but smaller than the second (1730 LST) on late double days. Early single days feature much larger rain rate than late single days. The second pulse in late double days seems to be more intense than second pulse in early double days, but the error bars are large to draw a definitive conclusion. The low-level cloud fraction is larger on early onset days than on late onset days with a diurnal maximum around 1330 LST for each category except that of late single days reaching the maximum value at 1530 LST. Note that rain rate here refers to the domain-mean value, whereas cloud

fraction is recorded by a single-point vertically pointing radar, the relationship between cloudiness and rain rate can vary with the clustering state of convective cells.

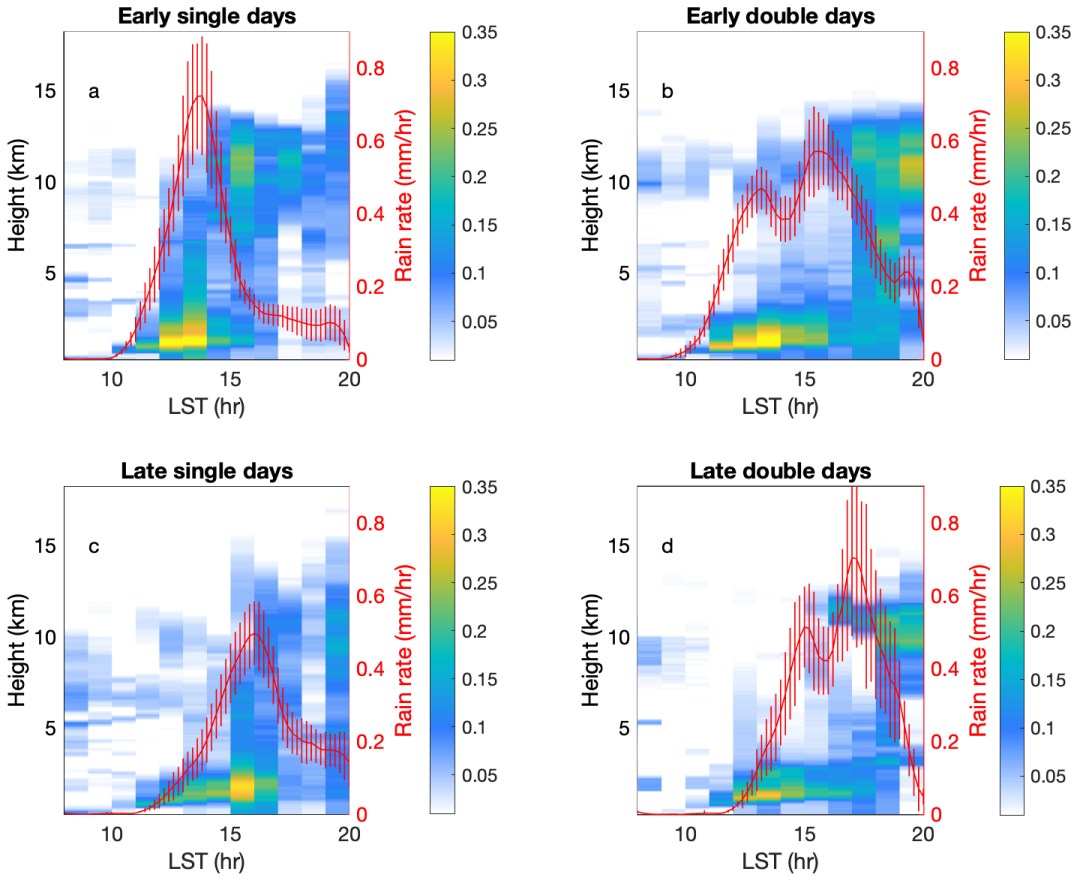

Fig. 1 Diurnal cycle of cloud fraction (color contour) and the domain-averaged rain rate (mm/hr) (red curves with values on the right Y-Axis). The vertical lines denote two standard errors.

2.3 Cluster tracking algorithm

Using scanning radar reflectivity, convective cloud clusters are defined as the areas of contiguous vertical columns with reflectivity above 10 dBZ for at least one level within each vertical column. A tracking algorithm is developed to explicitly reveal the evolution of each convective cluster within the analysis domain, e.g., from the first precipitation pulse to the second on the early double days. All the

details of this tracking algorithm are described in the supplemental materials, which include tracking steps, actions of clusters, parameters and sensitivity tests.

3 Results and discussions

3.1 Environmental conditions

In this section, we examine atmospheric moisture and instability, surface fluxes, and boundary layer thermodynamics, and how they vary between early and late onset days, as well as single and double pulse days.

Comparison between the days with an early or late precipitation onset

Between the early and the late precipitation onset days, are there any differences in the large-scale environmental conditions? Here early precipitation onset days include both early single and early double days (and likewise for late onset days). Figs. 2a and 2b show the 0800 LST sounding composite of relative humidity (RH) and atmospheric stability (the stratification of layer-mean potential temperature, $d\theta/dz$). A significant RH difference exists, where the late onset days are drier than the early days by 20% between 4-6 km. This dryness may limit the vertical development of convection; therefore, it may take longer for shallow clouds to grow deeper and precipitate. Besides, the early morning environment is more stable on the late onset days at 3-5 km than on the early onset days. While the difference is insignificant in surface latent heat fluxes (Fig. 2c), the late onset days have a larger surface sensible heat flux, thus also considered a contributor to the onset timing. These findings from GoAmazon are consistent with the ones on the isolated deep convections at the mid-latitude land by Zhang and Klein (2010) and many other studies (Del Genio 2012; Schiro et al. 2016; Itterly et al. 2016; Chakraborty et al. 2018), as well as convection studies over the Central Amazon (Williams et al. 2002;

Ghate and Kollias 2016; Giangrande et al. 2017; Zhuang et al. 2017; Marengo et al. 2017; Wang et al. 2018; Tian et al. 2021).

Comparison between the days with a single or double precipitation pulses

Given the limited number of late double days, the following discussion will focus on the comparison between the early single and the early double days, hereafter just called single and double days. To simplify, we call the precipitation pulse on the early single days as the single pulse, and the two precipitation pulses on the early double days as the first and the second pulse, respectively. In this section, we ask: Are there any significant differences in environmental conditions between the days with single and double precipitation pulses?

Figure 2d shows that at 0800 LST although the boundary layer RH is similar, RH at the 2.5-4 km on double days is about 15% lower than that on single days (Fig. 2d). Surface sensible heat flux on double days is about 50% larger than that on single days (Fig. 2e), which leads to a stronger entrainment and a slightly higher boundary layer top height (Fig. 2f). Due to the drier lower-free troposphere and the higher boundary layer top compared to single days, the initial development of deep convection may be prohibited on double days, which is consistent with the first-pulse rain rate on double days being much smaller than the single pulse on single days. Figure 2g shows that the CAPE around 1400 LST (after the first pulse but before the second pulse) on double days still maintains a high level, increasing the potential for a second round of convection.

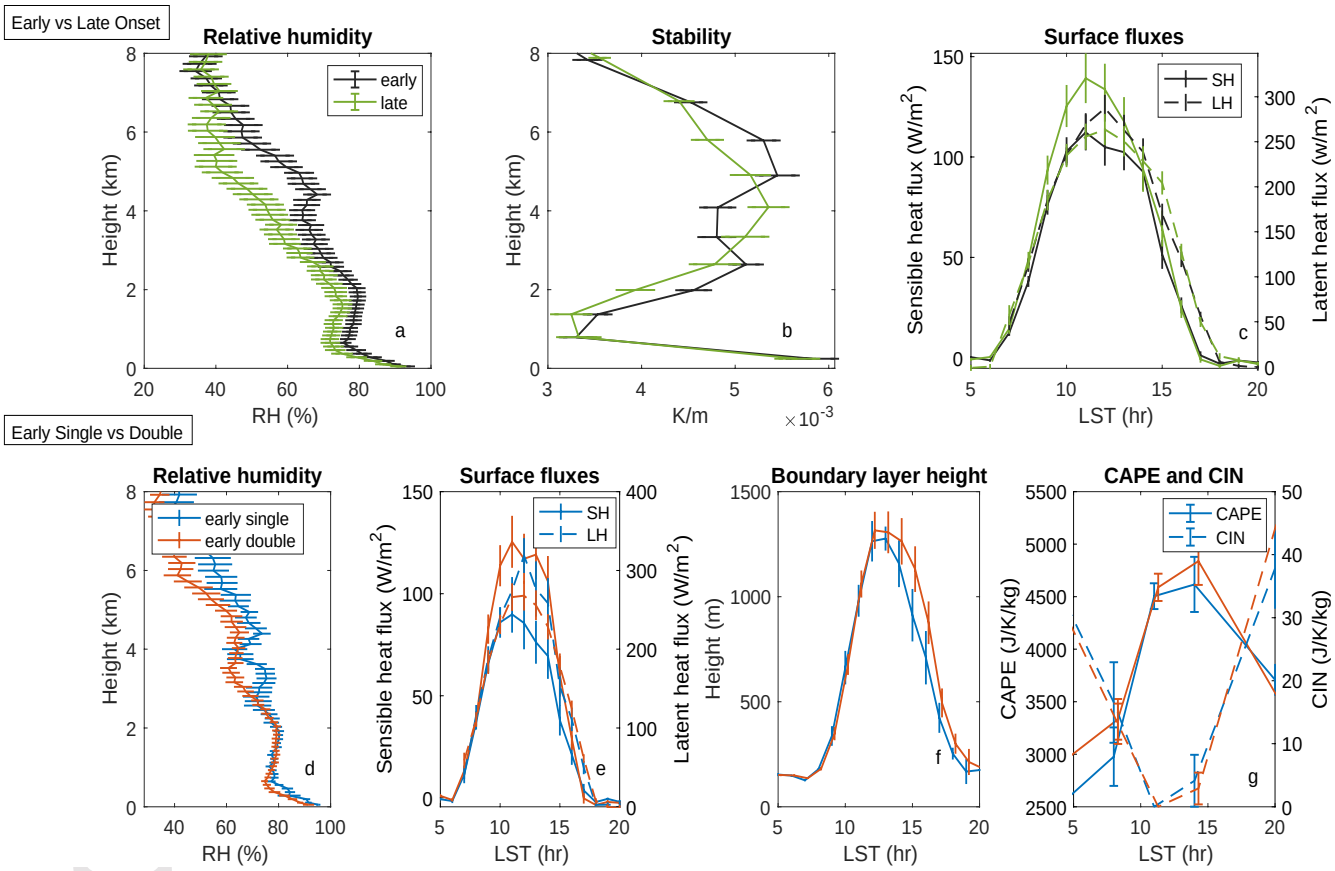

Fig. 2 (a)-(c) Relative humidity, atmospheric stability, and surface sensible (solid) and latent (dashed) fluxes on the early onset days (black) and the late onset days (green). (d)-(g) Relative humidity, surface sensible (solid) and latent (dashed) fluxes, boundary layer height, CAPE (solid, left Y-Axis) and CIN (dashed, right Y-Axis) on the early single days (blue) and the early double days (red). The length of the error bars denotes two standard errors.

3.2 Convective cluster characteristics

From Fig.1, with similar onset timing, the rain rate maximum value is significantly different between the single pulse on the early single days and the first pulse of the early double days. In this section, we ask: why is the rain rate of the single pulse significantly higher than that of the first pulse? Are there any differences in the cluster characteristics between the first pulse and the second on the double days? To answer these two questions, we investigate the characteristics of convective clusters explicitly. Based on the scanning precipitation radar reflectivity, we use two different thresholds to define a convective element: 10 dBZ for “cloud clusters” and 40 dBZ for “precipitation cores”. Figure

3 (a to d) shows the diurnal cycle of cloud number and cloud radius at 4 and 7 km altitudes. The choice of 4 and 7 km corresponds to the convective regime classification (Tian et al., 2021) in which cloud clusters with echo top lower than 4 km are defined as shallow cumulus, between 4 and 7 km as congestus, and reaching 7 km as deep convection. The cloud numbers are quite similar around 1300 LST, with the cloud radius even larger between 1100 and 1300 LST on the early double days. On double days, the cloud number initially decreases after the first pulse and then stabilizes at both altitudes of 4 and 7 km, while after a steady increase before the first pulse, the cloud radius experiences a rapid growth leading to the second pulse. This behavior of cloud clusters on early double days resembles that of a typical convective aggregation, in which the total number of cluster decreases, while the cluster size increases rapidly. We will return to this later and explore the possibility of convective aggregation using the tracking algorithm.

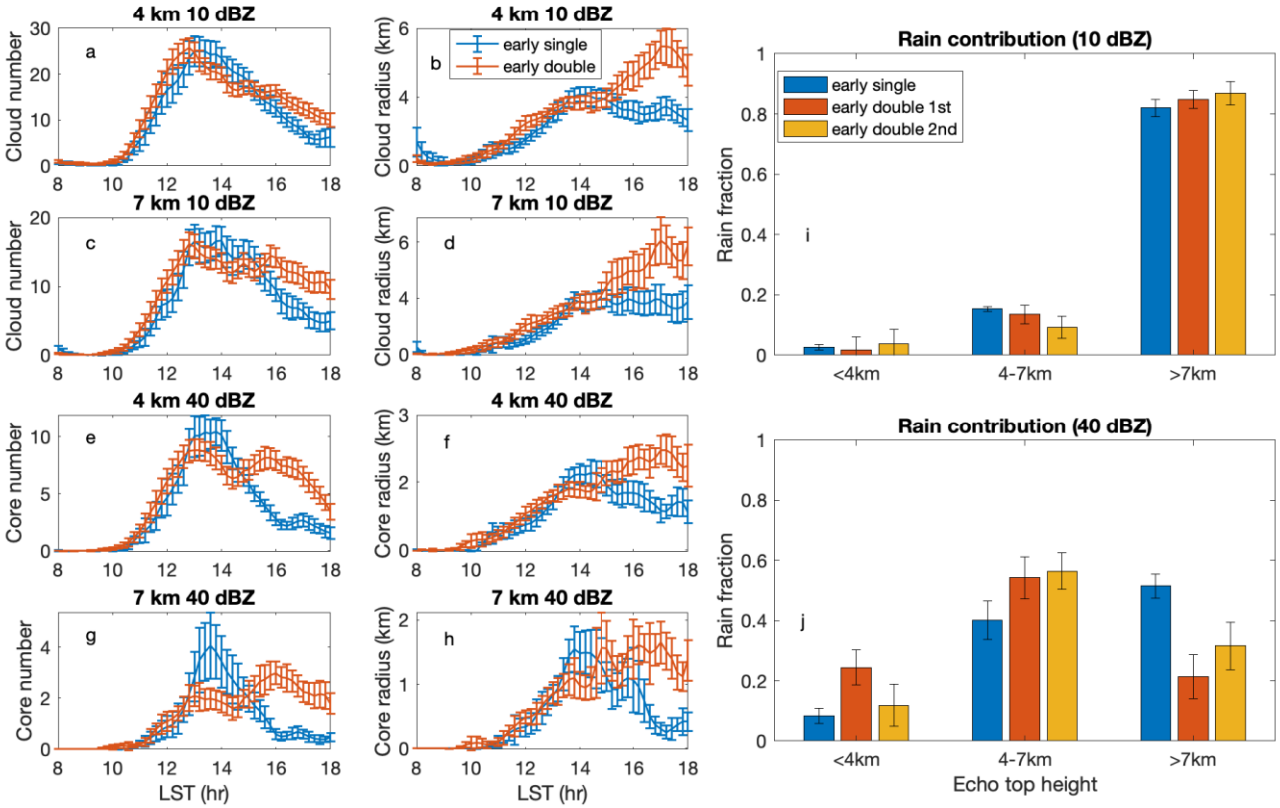

Fig. 3 (a)-(d) Diurnal cycle of cloud number and cloud radius reaching at 4 km and 7 km altitudes on the early single days (blue) and the early double days (red), where clouds are defined using a radar reflectivity threshold value of 10 dBZ; (e)-(h) Same as (a)-(d) but using a reflectivity threshold of 40 dBZ, which corresponds to the precipitation cores. The cloud (core) radius is calculated as the effective radius of a circle with the same area as the total number of vertical columns within each cloud (core) cluster. In (i) and (j), relative rain contribution is attributed to different cloud types with echo top heights < 4km, 4-7km, and >7km during the periods of the precipitation pulse on the early single days (blue), the first pulse (red), and the second pulse (orange) on the early double days, respectively. The length of the vertical bars denotes two standard errors.

Using 40 dBZ as precipitation cores, the signal of double precipitation pulses is more distinct, and the difference between single and double days is revealed more clearly, e.g., the core number (Fig. 3e & 3g). Around 1300 LST, even though the cloud number seems to be quite similar between single and double days, the actual precipitation core number differs drastically, especially those cores reaching above 7 km. This demonstrates that the precipitation difference between the single pulse and the first pulse is mainly contributed by the different number of precipitation cores penetrating strongly to higher altitudes, and it is those cores that dominate the domain mean precipitation. At 7 km during the second pulse, the core number increases, and the core size is larger than the first pulse on the early double days and becomes comparable to that of the single pulse on the early single days.

To examine the rain contribution from different types of convective clusters, we sampled the rain contribution from clouds (Fig 3i) and precipitation cores (Fig. 3j) with different echo top heights: below 4 km, between 4 and 7 km, and above 7 km. The fraction from each height category is normalized by the total rain from clouds or precipitation cores, thus sums to "1" for each pulse period. Stronger and deeper precipitation cores dominate the single pulse more than the first pulse (Fig. 3j). Interestingly on double days, most precipitation comes from cores reaching between 4-7 km during the first pulse (54%) and the second pulse (56%) (Fig. 3j). However, going from the first to the second pulse, the precipitation

that comes from cores below 4 km decreases (24% to 12%), whereas that comes from cores above 7 km increases (22% to 32%).

Figure 3 validates our argument that the stronger precipitation of the single pulse from deeper convective cores leads to more consumption of CAPE, thus a more stable atmosphere in late afternoon on the single days, which prohibits the generation of a second round of active convection. On the early double days, the convective development is strongly limited by the free troposphere humidity, the precipitation amount of the first pulse is only 60% of the single pulse, thus a less consumption of CAPE, and a less stable atmosphere after the first pulse. In addition, the dominant convection/precipitation below 4 km and between 4 to 7 km of the first pulse may help prepare a moister environment due to detrainment. All these factors give a rise to the generation of a second pulse.

What is the relationship of convective clusters between the first and the second pulse? In particular, can the evolution of convective clusters in Fig. 3, such as double pulses, be attributed to the interaction of clusters through convective aggregation? Or are the evolutions of convective clusters due to natural selection of more favorable convective clusters? To address these questions, we use the tracking algorithm to explicitly reveal the lifecycle of clusters and use an "encounter probability" metric to demonstrate the relative importance of different cluster behaviors. Encounter probability is defined as the forward-tracking probability (Fig. 4a) that a cluster, which exists during the first peak, will survive, and contribute to the second precipitation peak through a certain action. Analogously, the backward-tracking probability (Fig. 4b) is the probability that a cluster, which exists during the second peak, can be traced back to its origin at the first peak through a certain action. Figure 4a shows the encounter probability of convective clusters at the first pulse being forward tracked to the second pulse. It answers the question "What subsequently happens to the clusters identified at the initial pulse?" The probability is further partitioned by the initial cluster size at the first pulse and the five dominant actions

along the track of clusters: merging, splitting, growth, decay, and dissipation. Figure 4b shows the encounter probability of convective clusters at the second pulse being backward tracked to the first pulse, which is partitioned by the final cluster size at the second pulse and the dominant actions along the tracks. Figure 4b answers: "what previously happened to clusters in the second pulse?" There are seven actions in the calculation of encounter probability in Fig. 4a and 4b. Except the five dominant ones shown, two other actions not shown are advection and merging + splitting (both merging and splitting found on the same track). The action of advection is not sensitive to the cluster size. The probability for the action of merging + splitting to happen for a given track is low (<5%) among all tracks. Note that the "dissipation" or "generation" correspond to cases where a cluster cannot be tracked forward or backward to the other peak, thus should just be treated as probability rather than encounter probability.

In Fig. 4, the encounter probability decreases as a function of the initial cluster size during the first pulse in the action category of natural growth, however, increases in the category of decay. This suggests that if the convective cluster is already large enough at the first pulse, it is least likely for such cluster to persist until the second pulse by its own development without interacting with other clusters. Similarly, if the initial cluster size is too small, it is less likely for the cluster to survive long enough until the second pulse. The larger the initial cluster size, the more likely it lives up to the second pulse through merging with other convective clusters. Around 30-40% of the total clusters dissipate after the first precipitation pulse. In addition, it is rare for initial clusters to sustain to the second pulse through the action of splitting. It is interesting to note that with cluster size below 6 km, the probability of dissipation increases with cluster size, but decreases above, whereas the probability of merge increases.

This indicates that if the initial cluster size is above 6 km, it is more likely to interact with other clusters through merging.

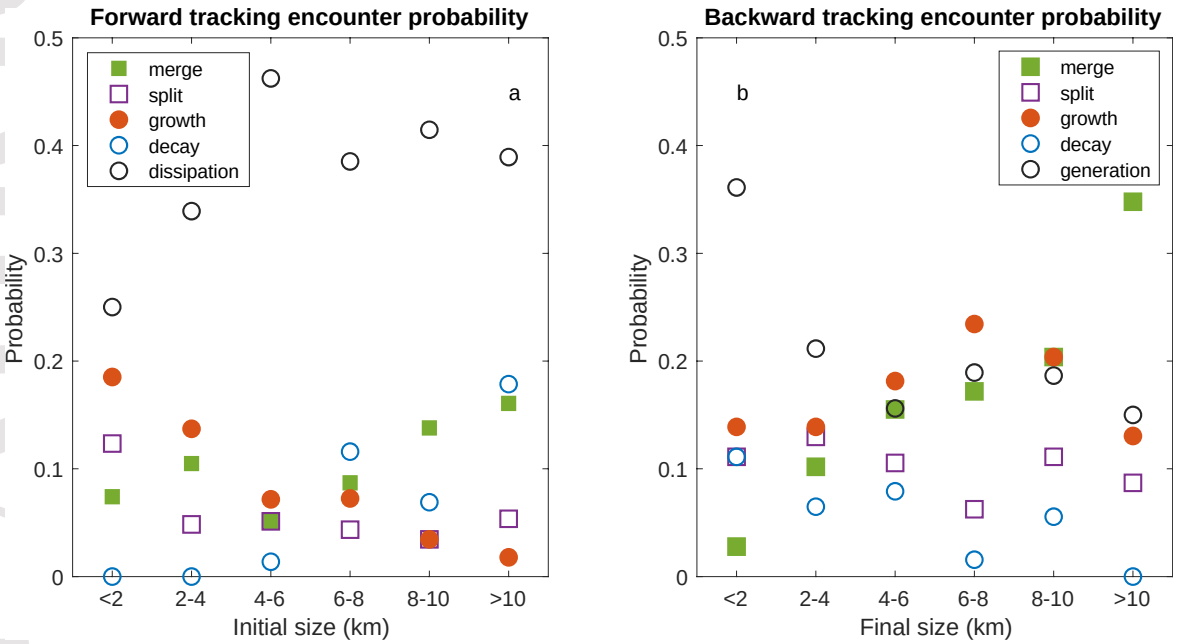

Fig. 4 Encounter probability of convective clusters between the two precipitation pulses on early double days. (a) Forward tracking from the first precipitation pulse to the second and the X-Axis shows the initial cluster size bins around the first pulse. (b) Backward tracking from the second precipitation pulse to the first, and the X-Axis shows the final cluster size bins around the second precipitation pulse. The cluster size is calculated as the effective radius of a circle with the same area as that of each cluster. The probability is attributed to different actions of the clusters evolving from the first to the second pulse: decay (blue open circle), growth (red solid circle), split (purple open square) and merge (green solid square), dissipation (open black circle in a) and new generation (open black circle in b).

If we bin the clusters by their final size at the second precipitation pulse and track their evolution backwards in time, the larger the final cluster size at the second pulse, the more likely it evolves from merging activity, e.g., in the bin with the largest final cluster size, 35% of the clusters evolves from merging. The natural growth contributes to approximately 20% of the encounter probability, which varies only slightly with the final size of clusters. In addition, the larger the final cluster size, the less likely the cluster evolves from a new generation in the analysis domain.

Figure 4 illustrates the tight relationship between the first and the second precipitation pulse on early double days. The first precipitation pulse sets the stage for the aggregation of convective clusters,

which becomes larger in size and precipitate more heavily during the second pulse. There can be a few mechanisms associated with this convective aggregation or cluster-cluster interaction. The aggregation occurs where several nearby independent clusters move close to each other and merge to form a much larger one (Muller and Bony 2015); the relatively weak convective clusters (congestus) pre-moisten the environment, which reduces the entrainment drying of the environment and promote the growth of larger clusters (Arnold and Randall 2015); the precipitation-driven cold pool provides strong mechanical lifting for air parcels to become freely-convecting and form more intense convective clusters (Torri et al. 2015); or the feedbacks between moisture aggregation and convection as discussed in Bretherton and Blossey (2017). *In summary, this cluster-cluster interaction can be important in determining the diurnal cycle of precipitation, therefore should be considered in designing convective schemes.*

In addition to the abovementioned cluster-cluster interaction, it is interesting to investigate if there can be any general synthesis that shows the relationship between free troposphere humidity, surface fluxes and cloud/precipitation type. Based on earlier discussion, free troposphere humidity controls both precipitation onset timing and the number of pulses on the early days, thus humidity and surface fluxes are shown for shallow cumulus days (defined in Tian et al. 2021), late precipitation onset days, early double days, and early single days in Fig. 5(a)-(b). Fig. 5(a) demonstrates a progression of humidity increasing at different height levels on the four types of convection days, e.g., the humidity difference becomes more significant from boundary layer to mid-troposphere. Another interesting finding is that the mid-level free troposphere humidity is anti-correlated with the surface sensible heat flux and downward shortwave radiation (Fig. 5b). It is possible that as mid-level humidity increases, the

surface downward solar radiation decreases both due to more water vapor and cloud cover (Fig. 5b), which would then decrease the sensible heat flux at the surface.

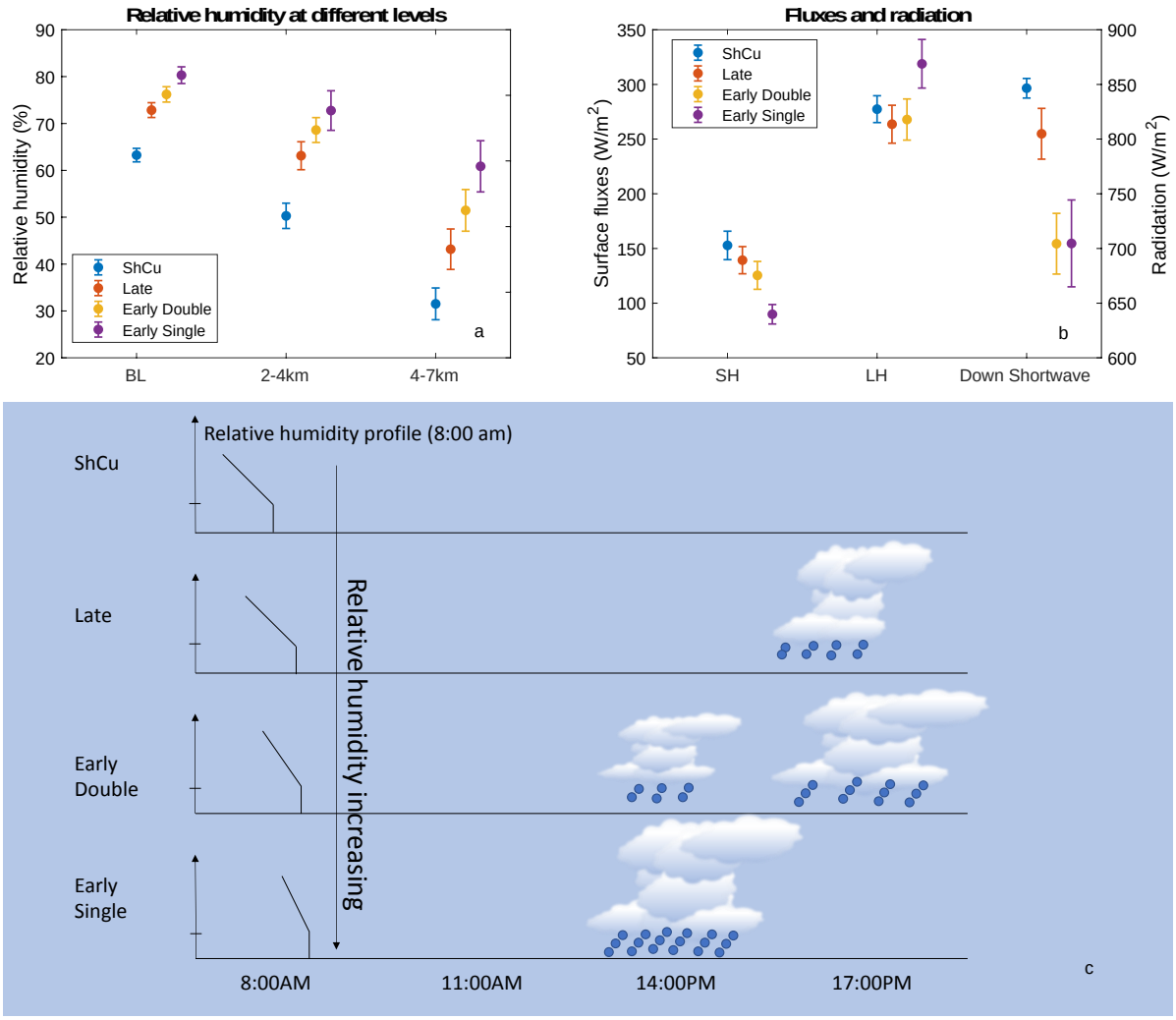

Fig. 5 (a) Layer-averaged relative humidity from 0800 LST sounding and (b) Diurnal maximum surface sensible and latent fluxes (left Y-Axis) and downward shortwave radiation (right Y-Axis) on the shallow cumulus days (blue), the late precipitation onset days (red), the early double days (orange) and the early single days (purple), the length of the vertical bars represents two standard errors; (c) A schematic generalizes the progression of cloud/convection diurnal patterns (from top to bottom) under the influence of an increasing early morning relative humidity. The geometry of convective clusters and their precipitation intensity are symbolized by the width and the vertical extent of the cartoon clouds and the density of blue dots.

Fig. 5(c) shows a schematic of the relationship between the early morning relative humidity and the cloud/precipitation types. The underlying mechanism to explain the trend in Fig. 5(a) is that if the

early morning relative humidity is too low, there will be no deep convection as on shallow cumulus days. As humidity increases slightly compared to shallow days, the precipitation tends to occur in the late afternoon, as humidity increases further, there will be early afternoon deep convection with a suppressed first pulse in the early afternoon and another intensified second pulse in the late afternoon, and as humidity increases even more, there only exists one single pulse in the early afternoon, which is so strong to consume available instabilities thus inhibits a second pulse of deep convection (Fig. 5c). Based on the analysis of the occurrence of those four convective types in wet and dry season, early onset days tend to occur more frequently in wet seasons than late onset days, and shallow days have clear preference over dry seasons, which indicates the influence of seasonal variation on the distribution.

4 Conclusions

Using the ARM GoAmazon observations, this work addresses an interesting new phenomenon in the diurnal cycle of precipitation over the tropical rainforest: on locally generated deep convection days, two precipitation pulses (usually two hours apart) are observed rather than one, which is rarely discussed in previous observational studies. The primary focus of this work is on a mechanistic understanding of the controlling factors of local double-pulse events from a diurnal cycle perspective. These controlling factors can be influenced by seasonal variation and large-scale circulation.

We categorize locally generated deep convection days into early versus late precipitation onset days. It is shown that atmospheric humidity in the early morning plays a critical role in determining the precipitation onset timing, which is consistent with most earlier studies.

Among these two broad categories of onset timing, days are further divided into single pulse versus double pulse days. Our analysis is focused on early onset days, and do not suggest explicitly that the same conclusion applied to late onset days. Even though the cloud cluster number and size do not

differ much between the single pulse on the early single days and the first pulse on the early double days, the precipitation of the single pulse almost doubles the amount of the first pulse on the early double days. On the early single days, the precipitation cores are more protected from entrainment drying due to a much moister early morning environment, thus penetrate to a much higher level than 7 km and precipitate more heavily. After heavy precipitation, atmosphere gets strongly stabilized and prohibits the further development of convective clusters, therefore only one pulse occurs during these days. On the first pulse of the early double days, a larger percentage of precipitation comes from the shallow and congestus clouds, and less from deep precipitating cores when compared to single pulse days. With weaker and shallower precipitation, the atmosphere remains less stable. In addition, the formation and dissipation of shallow and congestus clouds can probably contribute to a gradual moistening of the lower and middle troposphere, which favors the further development of deeper convection. After the first precipitation pulse, in addition to natural growth, convective clusters aggregate to form even larger and deeper clusters, which also adds to a stronger second precipitation pulse than the first pulse.

In our study, a tight relationship is observed between mid-level relative humidity and the precipitation onset timing as well as the number of pulses during daytime, whereas sensible fluxes show an opposite response. The results here confirm that the interaction among different convective clusters and the early morning free troposphere humidity can be important to influence the precipitation characteristics, therefore should be accounted for in the future convective scheme development.

Acknowledgments

The authors thank the U.S. Department of Energy (DOE)'s Atmospheric Radiation Measurement (ARM) data facility and the GoAmazon 2014/5 Field campaign. All the data used in this research are publicly available at https://www.arm.gov/research/campaigns/amf2014goamazon. The authors sincerely thank Courtney Schumacher from Texas A&M for the SIPAM S-band precipitation radar data and discussions on the tracking algorithms. Y. Tian, Y. Zhang, and S. A. Klein acknowledges support by the DOE's Atmospheric System Research (ASR), an Office of Science, Office of Biological, and Environmental Research program. Lawrence Livermore National Laboratory is operated for the DOE by Lawrence Livermore National Security, LLC under contract DE-AC52-07NA27344.

References

Arnold, N. P., and D. A. Randall (2015), Global-scale convective aggregation: Implications for the Madden-Julian Oscillation, J. Adv. Model. Earth Syst., 7, 1499– 1518. https://agupubs.onlinelibrary.wiley.com/doi/10.1002/2015MS000498

Bechtold, P., Chaboureau, J.-P., Beljaars, A., Betts, A. K., Köhler, M., Miller, M., & Redelsperger, J.-L. (2004). The simulation of the diurnal cycle of convective precipitation over land in a global model. Quarterly Journal of the Royal Meteorological Society, 130(604), 3119–3137. https://doi.org/10.1256/qj.03.103

Betts, A. K., and C. Jakob (2002). Evaluation of the diurnal cycle of precipitation, surface thermodynamics, and surface fluxes in the ECMWF model using LBA data. J. Geophys. Res., 107, 8045, https://doi.org/10.1029/2001JD000427.

Blekhman, A. (2021). An Intuitive Introduction to Kalman Filter (https://www.mathworks.com/matlabcentral/fileexchange/13479-an-intuitive-introduction-to-kalman-filter), MATLAB Central File Exchange.

Bretherton, C. S., & Blossey, P. N. (2017). Understanding mesoscale aggregation of shallow cumulus convection using large-eddy simulation. Journal of Advances in Modeling Earth Systems, 9, 2798–2821. https://doi.org/10.1002/2017MS000981

Chakraborty, S., Schiro, K. A., Fu, R., and Neelin, J. D. (2018). On the role of aerosols, humidity, and vertical wind shear in the transition of shallow-to-deep convection at the Green Ocean Amazon 2014/5 site, Atmos. Chem. Phys., 18, 11135–11148, https://doi.org/10.5194/acp-18-11135-2018, 2018.

Christopoulos, C., & Schneider, T. (2021). Assessing biases and climate implications of the diurnal precipitation cycle in climate models. Geophysical Research Letters, 48, e2021GL093017.

Clark P, Roberts N, Lean H, Ballard SP, Charlton-Perez C. (2016). Convection-permitting models: A step-change in rainfall forecasting. Meteorol. Appl. 23: 165–181, doi:10.1002/met.1538.

Covey, C., P. J. Gleckler, C. Doutriaux, D. N. Williams, A. Dai, J. Fasullo, K. Trenberth, and A. Berg (2016). Metrics for the diurnal cycle of precipitation: Toward routine benchmarks for climate models. J. Climate, 29, 4461–4471, https://doi.org/ 10.1175/JCLI-D-15-0664.1.

Collier, J. C., and K. P. Bowman (2004). Diurnal cycle of tropical precipitation in a general circulation model, J. Geophys. Res., 109, D17105, doi:10.1029/2004JD004818.

Dai, A., & Trenberth, K. E. (2004). The diurnal cycle and its depiction in the community climate system model. Journal of Climate, 17(5), 930–951. https://doi.org/10.1175/1520-0442(2004)0170930:TDCAID2.0.CO;2

Del Genio, A.D. (2012). Representing the sensitivity of convective cloud systems to tropospheric humidity in general circulation models. Surv. Geophys., 33, 637-656, doi:10.1007/s10712-011-9148-9.

Flato, G., and Coauthors (2014). Evaluation of climate models. Climate Change 2013: The Physical Science Basis, T. F. Stocker et al., Eds., Cambridge University Press, 741–866.

Ghate, V. P., & Kollias, P. (2016). On the Controls of Daytime Precipitation in the Amazonian Dry Season. Journal of Hydrometeorology, 17(12), 3079–3097. https://doi.org/10.1175/JHM-D-16-0101.1

Giangrande, S. E., Toto, T., Jensen, M. P., Bartholomew, M. J., Feng, Z., Protat, A., et al. (2016). Convective cloud vertical velocity and mass- flux characteristics from radar wind profiler observations during GoAmazon2014/5. Journal of Geophysical Research: Atmospheres, 121(21), 12891–12913. https://doi.org/10.1002/2016JD025303

Giangrande, S. E., Feng, Z., Jensen, M. P., Comstock, J. M., Johnson, K. L., Toto, T., et al. (2017). Cloud characteristics, thermodynamic controls and radiative impacts during the Observations and Modeling of the Green Ocean Amazon (GoAmazon2014/5) experiment. Atmospheric Chemistry and Physics, 17(23), 14519–14541. https://doi.org/10.5194/acp-17-14519-2017

Guichard, F., Petch, J. C., Redelsperger, J. L., Bechtold, P., Chaboureau, J. P., Cheinet, S., et al. (2004). Modeling the diurnal cycle of deep precipitating convection over land with cloud-resolving models and single-column models. Quarterly Journal of the Royal Meteorologi- cal Society, 130(604), 3139–3172. https://doi.org/10.1256/qj.03.145

Holloway, C.E., Wing, A.A., Bony, S. et al. Observing Convective Aggregation. Surv Geophys 38, 1199–1236 (2017). https://doi.org/10.1007/s10712-017-9419-1

Huang, X. M., Hu, C. Q., Huang, X., Chu, Y., Tseng, Y., Zhang, G. J., & Lin, Y. L. (2018). A long term tropical mesoscale convective systems dataset based on a novel objective automatic tracking algorithm. Climate Dynamics, 51, 3145–3159. https://doi.org/10.1007/s00382- 018-4071- 0

Itterly, K. F., P. C. Taylor, J. B. Dodson, and A. B. Tawfik (2016). On the sensitivity of the diurnal cycle in the Amazon to convective intensity, J. Geophys. Res. Atmos., 121, 8186–8208, doi:10.1002/ 2016JD025039.

Lee, M. I., Schubert, S. D., Suarez, M. J., Schemm, J. K. E., Pan, H. L., Han, J., & Yoo, S. H. (2008). Role of convection triggers in the simulation of the diurnal cycle of precipitation over the United States Great Plains in a general circulation model. Journal of Geophysical Research Atmospheres, 113(2), 1–10. https://doi.org/10.1029/2007JD008984

Marengo, J.A., Fisch, G.F., Alves, L.M., et al., 2017. Meteorological context of the onset and end of the rainy season in Central Amazonia during the GoAmazon2014/5. Atmospheric Chemistry and Physics, 17(12), pp.7671-7681.

Muller, C. and S. Bony (2015). "What favors convective aggregation, and why?" Geophysical Research Letters 42: 5626-5634.

Pearson, K. J., G. M. S. Lister, C. E. Birch, R. P. Allan, R. J. Hogan, and S. J. Woolnough (2014). Modelling the diurnal cycle of tropical convection across the 'grey zone.' Quart. J. Roy. Meteor. Soc., 140, 491–499, https://doi.org/10.1002/qj.2145.

Prein, A. F., et al. (2015), A review on regional convection-permitting climate modeling: Demonstrations, prospects, and challenges, Rev. Geophys., 53, 323–361, doi:10.1002/2014RG000475.

Rosa, D., and W. Collins (2013). A case study of subdaily simulated and observed continental convective precipitation: CMIP5 and multiscale global climate models comparison. Geophys. Res. Lett., 40, 5999–6003, https://doi.org/10.1002/2013GL057987.

Sato, T., Miura, H., Satoh, M., Takayabu, Y. N., & Wang, Y. (2009). Diurnal cycle of precipitation in the tropics simulated in a global cloud-resolving model. Journal of Climate, 22(18), 4809–4826. https://doi.org/10.1175/2009JCLI2890.1

Schumacher, C., & Funk, A. (2018). GoAmazon2014/5 Three-dimensional Gridded S-band Reflectivity and Radial Velocity from the SIPAM Manaus S-band Radar. United States. https://doi.org/10.5439/1459573

Stull, R. (2017). Chapter 14 Thunderstorm fundamentals. Practical meteorology: An algebra-based survey of atmospheric science. Springer.

Schiro, K. A., Neelin, J. D., Adams, D. K., & Lintner, B. R. (2016). Deep convection and column water vapor over tropical land versus tropi- cal ocean: A comparison between the Amazon and the tropical western Pacific. Journal of the Atmospheric Sciences, 73(10), 4043–4063. https://doi.org/10.1175/JAS-D-16-0119.1

Schlemmer, L., Hohenegger, C., Schmidli, J., Bretherton, C., & Schär, C. (2011). An idealized cloud resolving framework for the study of summertime midlatitude diurnal convection over land. Quarterly Journal of the Royal Meteorological Society, 68(5), 1041–1057. https:// doi.org/10.1175/2010JAS3640.1

Tian, Y., Zhang, Y., Klein, S. A., & Schumacher, C. (2021). Interpreting the diurnal cycle of clouds and precipitation in the ARM GoAmazon observations: Shallow to deep convection transition. Journal of Geophysical Research: Atmospheres, 126, e2020JD033766. https://doi. org/10.1029/2020JD033766

Torri, G., Kuang, Z., & Tian, Y. (2015). Mechanisms for convection triggering by cold pools. Geophysical Research Letters, 42(6), 1943–1950. https://doi.org/10.1002/2015GL063227

Wang, D., Giangrande, S. E., Bartholomew, M. J., Hardin, J., Feng, Z., Thalman, R., & Machado, L. A. T. (2018). The Green Ocean: Precipi- tation insights from the GoAmazon2014/5 experiment. Atmospheric Chemistry and Physics, 18(12), 9121–9145. https://doi.org/10.5194/ acp-18-9121-2018

Williams, E., Rosenfeld, D., Madden, N., et al., 2002. Contrasting convective regimes over the Amazon: Implications for cloud electrification. Journal of Geophysical Research: Atmospheres, 107(D20), pp.LBA-50.

Xie, S., and Coauthors (2019). Improved diurnal cycle of precipitation in E3SM with a revised convective triggering function. J. Adv. Model. Earth Syst., 11, 2290–2310, https://doi.org/ 10.1029/2019MS001702.

Yang, G.-Y., & Slingo, J. (2001). The diurnal cycle in the tropics. Monthly Weather Review, 129(4), 784–801. https://doi.org/10.1175/1520-0493(2001)129<0784:TDCITT>2.0.CO;2

Yin, J., & Porporato, A. (2017). Diurnal cloud cycle biases in climate models. Nature Communications, 8(1), 2269. https://doi.org/10.1038/s41467-017-02369-4

Zhang, Y. Y., & Klein, S. A. (2010). Mechanisms affecting the transition from shallow to deep convection over land: Inferences from observations of the diurnal cycle collected at the ARM Southern Great Plains site. Journal of the Atmospheric Sciences, 67(9), 2943–2959. https://doi.org/10.1175/2010JAS3366.1

Zhuang, Y., Fu, R., Marengo, J.A., et al., 2017. Seasonal variation of shallow- to- deep convection transition and its link to the environmental conditions over the Central Amazon. Journal of Geophysical Research: Atmospheres, 122(5), pp.2649-2666.